Scientific paper

Synthesis, Crystal Structure and In Vitro Cytotoxicity of Novel Cu(II) Complexes Derived from Isatin Hydrazide-Hydrazone Ligands

Cansu Topkaya*

Muğla Sıtkı Koçman University, Department of Chemistry, 48000 Muğla, Turkey

** Corresponding author: E-mail: cansutopkaya@mu.edu.tr*
Phone: +90 252 2111502, fax: +90 252 2111472

Received: 08-17-2023

Abstract

In this study, two innovative hydrazine-hydrazone ligands were synthesized through the chemical reaction involving the isatin moiety with 4-hydroxybenzohydrazide and salicyloylhydrazine. Subsequent to the synthesis of these ligands, Cu(II) complexes were meticulously prepared, and their molecular structures were comprehensively analyzed utilizing an array of spectroscopic techniques. Furthermore, the crystallographic investigation was employed to elucidate the precise crystal structure of the $Cu(L^2)_2$ complex, incorporating the salicyloylhydrazine moiety. The research focuses on investigating the cytotoxic effects of Cu(II) complexes bearing isatine groups on cancer cells. These complexes were tested against lung carcinoma (A549) and breast carcinoma (MCF-7) cell lines using the MTT assay, with cisplatin as a positive control. Additionally, their effects on human normal cell line 3T3 were assessed. The $Cu(L^1)_2$ complex exhibited significant inhibitory effects on tumor cells in a dose-dependent manner, although not as potent as cisplatin. The cytotoxic selectivity indices (SI) indicated acceptable selectivity levels for both cancer cell lines, indicating potential for selective lethality. The crystal structure of one compound was confirmed, revealing van der Waals interactions and hydrogen bonding in the packing.

Keywords: Isatin; hydrazone; metal complexes; crystal structure; cytotoxic activity.

1. Introductıon

Isatin and its derivatives hold significant importance in the field of inorganic chemistry and encompass diverse applications. Isatin serves as a versatile ligand for metal complexes, exerting a profound influence on the synthesis of catalysts, photosensitizers, electrochromic materials, and bioactive compounds. Notably, isatin derivatives have attracted considerable attention in the pharmaceutical industry, showcasing a spectrum of biological activities encompassing anticancer, antiviral, and antimicrobial properties. Moreover, isatin and its derivatives find utility in molecular labeling, sensor technologies, and the realm of biological imaging. Within the domain of inorganic chemistry, the incorporation of isatin and its derivatives as ligands enables investigations into metal complexes, contributing substantially to a broad range of applications.[1,2]

Hydrazide-hydrazone derivatives, distinguished by their unique reactive moiety (CO-NH-N=CH), have emerged as highly promising candidates in the realm of novel drug development. These compounds have garnered substantial recognition within the field of medicinal chemistry owing to their multifaceted biological properties. Notably, they have exhibited significant potential in various therapeutic areas, encompassing antimicrobial, anti-mycobacterial, anticonvulsant, analgesic, anti-inflammatory, anti-platelet, anti-tubercular, anti-tumoral, anti-cancer, and anti-HIV activities. The remarkable breadth of their potential applications underscores the growing significance and versatility of hydrazide-hydrazones in the realm of medicinal chemistry.[3–6]

Hydrazide-hydrazone derivatives have demonstrated versatility in coordinating with metal ions, leading to the formation of metal complexes. These complexes exhibit unique properties and biological activities, making them valuable in catalysis, medicinal chemistry, and materials science. The coordination of metal ions with hydrazide-hydrazones allows for the manipulation of reactivity and stability, expanding their potential applications.

These metal complexes also show promise as antibacterial, antifungal, and anticancer agents, highlighting their potential in therapeutic interventions. Overall, exploring metal complexes of hydrazide-hydrazones offers opportunities for designing novel compounds with enhanced characteristics.[7–9]

Copper holds a pivotal role as an essential bioelement within various biological systems, influencing a wide array of physiological activities and cellular mechanisms. Its significance extends to human metabolism, where it plays a crucial part in enzymatic reactions and cellular processes. Furthermore, copper's importance isn't confined solely to biological functions; it also extends to the development of pharmaceutical agents with therapeutic applications. This dual role, both as a biological necessity and as a key element in pharmaceutical research, underscores the multifaceted importance of copper in the realms of biology and medicine.[10–12]

This study focuses on the synthesis and characterization of new hydrazide-hydrazone derivatives containing isatin groups and their corresponding Cu(II) complexes. The molecular structures of the compounds were investigated using various spectroscopic techniques, and the one of Cu(II) complexes was further characterized by single crystal X-ray diffraction (XRD) analysis. Additionally, the synthesis of a series of hydrazide-hydrazone compounds and the subsequent evaluation of their Cu(II) complexes were carried out with the objective of obtaining novel anticancer agents.

2. Experimental

2. 1. Materials and Measurements

Solvents and chemicals utilized in the laboratory were procured commercially from Merck and Sigma. Solvents employed in the synthesis and measurements were subjected to meticulous purification procedures involving distillation and drying. Microanalysis, specifically carbon (C), nitrogen (N), and hydrogen (H) analysis, was performed using an LECO 932 CHNS analyzer. The copper content was quantified employing atomic absorption spectroscopy on a DV 2000 Perkin Elber ICP-AES instrument. Thermo-Scientific Nicolet iS10-ATR infrared spectra were acquired using the attenuated total reflectance (ATR) method, spanning the wavenumber range from 4000 to 400 cm^{-1}. Magnetic susceptibility of powdered materials at ambient temperature was evaluated utilizing a Sherwood Scientific MK1 Model Gouy Magnetic Susceptibility Balance. Electronic spectra were recorded employing a PG Instruments T80+ UV/Vis Spectrophotometer. Notably, the compounds 4-hydroxybenzohydrazide (I)[13] and salicyloylhydrazine (II)[14] were synthesized according to the reported methodology. Crystallographic data were recorded on a Bruker APEX-II CCD diffractometer using MoK$_\alpha$ radiation (λ = 0.71073 Å).

2. 2. Synthesis and Characterization

Synthesis of Ligands: The synthesis of these compounds was accomplished by modifying the literature method.[15] A solution of 0.01 mol of 4-hydroxybenzohydrazide (HL^1) and salicyloylhydrazine (HL^2) in 15 mL of ethanol was prepared. Subsequently, a solution containing 0.01 mol of isatin in 10 mL of ethanol was added to the aforementioned solution. Following the completion of the addition, a few drops of acetic acid were introduced as a catalyst, and the reaction mixture was subjected to reflux conditions for approximately 5 hours. Initially, the solution exhibited clarity; however, over time, yellow solid precipitates began to form. The resulting yellow precipitates were isolated by filtration. The purity of the obtained product was assessed using thin-layer chromatography (TLC), and final purification was achieved through crystallization from a 1:1 ethanol-water mixture.

(E)-4-hydroxy-N'-(2-oxoindolin-3-ylidene)benzohydrazide (*HL^1*): Yield: 85 %; m.p. 259–262 °C. FT-IR (ATR, cm^{-1}): 3143 ν(N-OH), 1690;1656 ν(C=O), 1608 ν(C=N), 1265 ν(C-O); UV (EtOH, λ, nm): 220, 250, 274 (sh), 338,5, 404,5 (sh) ^{1}H NMR (400 MHz, DMSO_d^6, ppm) δ 13.87 (s, 1H, Ar-O*H*), 11.37 (s, 1H, N*H*), 10.31 (s, 1H, N*H*), 7.77 (t, 2H, Ar-*H*), 7.60 (t, 1H, Ar-*H*) 7.39 (q, 1H, Ar-*H*) 7.12 (q, 1H, Ar-*H*) 6.95 (m, 3H, Ar-*H*); Analysis (% calculated/found) for $C_{15}H_{11}N_3O_3$, C: 64.05/64.10, H: 3.94/3.95, N: 14.94/14.84.

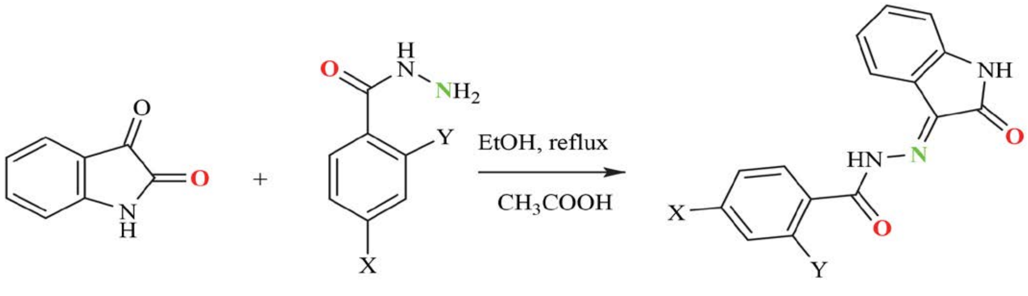

I and II

Scheme 1. Synthesis and proposed structure of hydrazone ligands (4-hydroxybenzohydrazide (HL^1) and salicyloylhydrazine (HL^2).

(E)-2-hydroxy-N'-(2-oxoindolin-3-ylidene)benzohydrazide *(HL^2)*: Yield: 80 %; m.p. 229–229 °C. FT-IR (ATR, cm^{-1}): 3156 ν(N-OH), 1740; 1667 ν(C=O), 1607 ν(C=N), 1236 ν(C-O); UV (EtOH, λ, nm): 209,5, 248, 338,5, 403(sh), ^1H NMR (400 MHz, DMSO_d^6, ppm) δ 14.38 (s, 1H, Ar-O*H*), 12.19 (s, 1H, N*H*), 10.90 (s, 1H, N*H*), 8.07 (d, 1H, Ar-*H*), 7.61 (d, 1H, Ar-*H*) 7.46 (d, 1H, Ar-*H*) 7.12 (d, 1H, Ar-*H*) 7.04 (d, 2H, Ar-*H*) 6.99 (t, 2H, Ar-*H*); Analysis (% calculated/found) for $C_{15}H_{11}N_3O_3$, C: 64.05/64.08, H: 3.94/3.90, N: 14.94/14.97.

Synthesis of Cu(II) Complexes: The synthesis procedure proceeded as follows: A suspension of 0.02 mol of the hydrazone ligand in ethanol was prepared, and subsequently, a solution of 0.01 mol of copper(II) acetate dihydrate in ethanol was added dropwise to the suspension. The resulting mixture was subjected to reflux conditions for approximately 2 hours, followed by cooling and filtration. The obtained solid was washed with alcohol and water, and then allowed to dry. Crystallization of the complexes was achieved using a mixture of dimethylformamide (DMF) and ether.

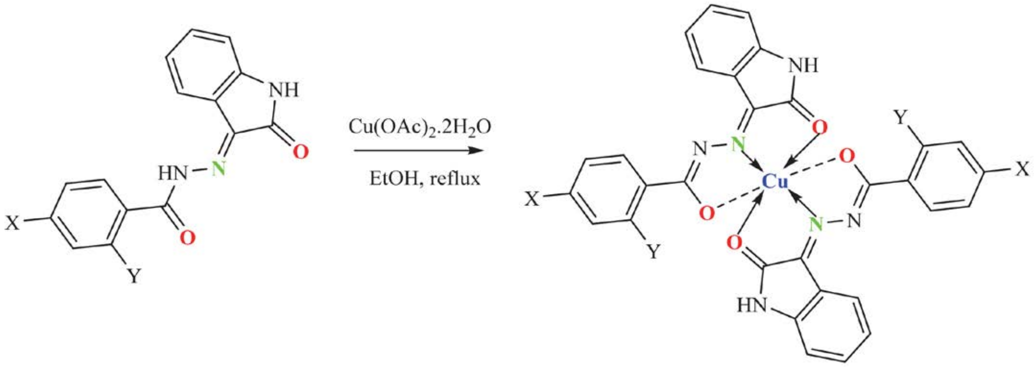

Scheme 2. Synthesis and proposed structure of Cu(II) complexes.

For Cu(L^1)$_2$: $C_{30}H_{20}CuN_6O_6.2H_2O$, Brown complex; Yield: 65 %; m.p.: >350 °C. μeff = 1.70 B.M.; UV-vis (EtOH, nm) 210,5, 250,0, 276,5 (sh); 363, 398 and 442 (sh). FT-IR (ATR, cm^{-1}) 3354 (OH), 1609 m (C=N-N=C), 1214 w (C–O). Analysis (% calculated/found) for $C_{30}H_{20}CuN_6O_6$, C: 54.59/54.60, H: 3.66/3.59, N: 12.73/12.44, Cu:9.63/9.41.

For Cu(L^2)$_2$: $C_{30}H_{20}CuN_6O_6.4H_2O$, Dark Brown complex; Yield: 67 %; m.p.: >350 °C. μeff = 1.69 B.M.; UV-vis. (EtOH, nm) 212,5, 250, 291,5, 361,5 (sh), 426,5 (sh). FT-IR (ATR, cm^{-1}) 3325 (OH), 1632–1604 m (C=N-N=C), 1213 w (C–O). Analysis (% calculated/found) for $C_{30}H_{20}CuN_6O_6$, C: 51.76/51.65, H: 4.05/4.07, N: 12.07/12.50, Cu: 9.13/9.25.

2. 3. X-ray Crystallography

Suitable crystal of Cu(L^2)$_2$ was selected for data collection which was performed on a Bruker diffractometer equipped with a graphite-monochromatic Mo-Kα radiation at 296 K. The structure was solved by direct methods using SHELXS-2013[16] and refined by full-matrix least-squares methods on F2 using SHELXL-2013.[17] The following procedures were implemented in our analysis: data collection: Bruker APEX2; [18] programs used for molecular graphics were as follow: MERCURY programs;[19] software used to prepare material for publication: WinGX.[20] Crystallographic data for the structure reported herein have been deposited with the Cambridge Crystallographic Data Centre as Supporting Information, CCDC No. **2288219**. Copies of the data can be obtained through application to CCDC, 12 Union Road, Cambridge CB2 1EZ, UK. (fax: +44 1223 336033 or e-mail: deposit@ccdc.cam.ac.uk or at http://www.ccdc.cam.ac.uk).

2. 4. Biological studies

Cell culture

Human cancer cell lines, breast cancer cell line (MCF-7) and lung carcinoma cell line (A549), human normal cell line [embryonic fibroblast cells (3T3)] were obtained from the European Collection of Cell Cultures (ECACC, UK). The cells were cultured under standard conditions in Dulbeccos' Modified Eagle Medium (DMEM) (Gibco, Invitrogen Inc., Carlsbad, California, USA), supplemented with 10% heat-inactivated fetal bovine serum (FBS) (Gibco, Invitrogen Inc., Carlsbad, California, USA), 100 U/mL of penicilin, and 100 U/ml of streptomycin and 4 mM L-glutamine, incubated in a humidified incubator set at 37 °C with 5% CO_2. The stock solution of the Cu(II) complexes (10 mM) was prepared in DMF (equivalent to < 0.5% of the final volume), while the clinically-used formulation of cisplatin (Cipintu, 100 mg/100 ml) was used as a stock solution. Further dilutions were made with cell culture medium.

Cell viability inhibition assay

3T3, A549 and MCF-7 cells (5x10^3 per well) seeded in 96-well plates to assess cell viability by the 3-[4,5-dimethylthiazol-2-yl]-2,5-diphenyltetrazolium bromide

(MTT) assay for 24 h at 37 °C. Then, cells were treated with Cu(II) complexes at different concentrations (7.5–250 μM) at 100 μl/well. Under the same settings, the standard anticancer drug cisplatin was utilized as a positive control. After 24, 48 and 72 h incubation, 5 mg/ml MTT solution (20 μl/well) was added and cultured for another 4 h. Then, the supernatant was discarded and dimethyl sulfoxide was added (100 μl/well). A Microplate Reader was used to measure the absorbance (A) spectrophotometrically at 540 nm (SpectraMax i3x). The concentrations of the compound were plotted against the percent viability on a graph. Graphs were used to calculate the concentrations of samples that inhibited the growth of 50% of the cells (IC_{50} values). All tests were run three times for each concentration level.[21]

3. Results and Discussion

3. 1. Characterization of the Compounds

According to the ^1H NMR spectra of the ligands, the proton adjacent to the imine group arising from the two -NH groups in the ligands' structure was observed at chemical shifts of 11.37 ppm and 12.19 ppm, respectively. The -NH group within the isatin ring exhibited signals at 10.31 ppm in the HL^1 ligand and at 10.90 ppm in the HL^2 ligand. The hydroxyl (-OH) peak of the ligand synthesized with 4-hydroxybenzohydrazide appeared at 13.87 ppm, while the -OH peak of the ligand synthesized with salicyloylhydrazine was observed at 14.38 ppm. The downward shift of the phenolic OH proton absorption can be attributed to the presence of strong intramolecular hydrogen bonding in these compounds.[22–24] The other proton resonances of these ligands are given experimental section.

Upon comparison of the FTIR spectra between the derivatives of 4-hydroxybenzohydrazide and salicyloylhydrazone, the stretching vibrations of the ν(C=O) in the HL^1 ligand were observed in the range of 1690–1656 cm^{-1}, whereas those in the H_2L^2 ligand appeared in the range of 1740–1667 cm^{-1}. This observation can be rationalized by the occurrence of intermolecular hydrogen bonding between the carbonyl groups of the salicyloylhydrazone derivatives and the phenolic -OH moiety. The hydroxyl groups within the ligand structure were detected at wavenumbers of 3143 cm^{-1} and 3156 cm^{-1}, respectively. Notably, the -NH stretching bands of these compounds could not be discerned in the IR spectra, most likely due to overlap with the -OH stretching frequencies. Additional distinctive IR peaks pertaining to the hydrazide-hydrazone compounds synthesized in this investigation are provided in the experimental section. These results are consistent with the previously reported hydrazone derivatives.[25–27]

The IR spectra of the complexes demonstrate notable distinctions when compared to those of the free ligands. Specifically, the characteristic bands associated with amide I vibrations of ν(C=O), imine ν(C=N) and amide vibrations of ν(NH) are not directly evident in the IR spectra of the complexes. Instead, the emergence of two new bands within the spectral range of 1609 cm^{-1} and 1632–1604 cm^{-1} is observed. These newly observed bands can be ascribed to the presence of C=N-N=C and C=O moieties, suggesting a perturbation in the coordination environment.

The absence of the -NH proton resonance in the IR spectra suggests the occurrence of enolization, leading to the relinquishment of the -NH proton. Consequently, the resulting enolic oxygen and azomethine nitrogen actively participate in coordination with the central metal. These findings align with prior investigations.[26,27] The observed upshift in the stretching vibration of the ν(N=N) in the complexes, by approximately 30–35 cm^{-1} compared to the free ligand, provides additional evidence supporting the involvement of the azomethine nitrogen in coordination. This shift to higher energy suggests a change in the bonding environment around the azomethine nitrogen upon coordination with the metal center. Such alterations in the vibrational frequencies can be indicative of the formation of a coordinate bond between the azomethine nitrogen and the metal atom. This observation further supports the proposition that the azomethine nitrogen actively participates in the coordination process in these complexes. In Cu(II) complexes, the symmetric and asymmetric stretching vibrations of the hydroxyl group ν(-OH) in hydrazide-hydrazone derivative ligands are observed, suggesting that they are not engaged in coordination. The IR spectra of these complexes exhibit a broad band around 3300 cm^{-1} for the 4-hydroxybenzohydrazide derivative and a narrower band for the salicyloylhydrazine derivative. This spectral observation can be attributed to the presence of intramolecular hydrogen bonding involving the phenolic -OH group.

Ligands and Cu(II) complexes exhibit an average of four or five electronic transitions in their electronic spectra. Absorbances occurring around 200–250 nm are presumed to be associated with $\pi \rightarrow \pi^*$ electronic transitions. The absorptions observed at around 290 nm and 350 nm correspond to $n \rightarrow \pi^*$ electronic transitions in the compounds. Furthermore, peaks above 400 nm in the complexes' spectra represent the peaks of d-d charge-transfer transitions of the complexes.[28,29]

The Cu(II) complex exhibits paramagnetic behavior at room temperature. The observed magnetic moment values for the mononuclear Cu(II) complexes were measured to be 1.70 BM and 1.69 BM, which falls within the expected range for mononuclear copper(II) complexes (1.73 BM) containing a single Cu(II) cation with a d^9 electronic configuration.[30] The magnetic data analysis reveals that mononuclear copper(II) complexes, which possess an octahedral coordination environment facilitated by the additional axial coordination of ligand molecules, adopt a high-spin configuration.

The thermograms of all Cu(II) complexes were recorded within a temperature range of 30 to 800 °C using a heating rate of 20 °C/min under a nitrogen atmosphere.

Above 900 °C, complete decomposition of the complexes was observed, as depicted in Figure S11-12. The decomposition step occurring around approximately 200 °C with an associated mass loss of about 5% for the $Cu(L^1)_2$ complex corresponds to the removal of two moles of water present in the structure. Furthermore, for the $Cu(L^2)_2$ complex, a similar decomposition stage initiates around 270 °C, indicating an approximate mass loss of 8%. This mass loss, equivalent to four moles of water, occurring at a higher temperature compared to $Cu(L^1)_2$ complex, can be attributed to its encapsulated nature within the crystal structure. The second decomposition stage, which commences at around 300 °C for all complexes, likely signifies the breakdown of all the complexes. This decomposition process culminates at a temperature of around 500 °C.

All spectral data are consistent with those reported for similar compounds.[25–27] Elemental analysis, UV-Vis, IR, ^{1}H-NMR and TGA analysis are confirmed the molecular formula.

3. 2. X-Ray Structure

The X-ray structural determination of title compound confirms the assignment of its structure from spectroscopic datas. As shown in Fig. 1, the compound consists of new hydrazide-hydrazone derivatives containing isatin and salicyloylhydrazine and its Cu(II) complexes. The experimental details are given in Table 1. Hydrogen bond

Table 1. Experimental details.

Crystal data	
Chemical formula	$C_{30}H_{20}CuN_6O_6{\cdot}4(H_2O)$
M_r	696.12
Crystal system, space group	Monoclinic, C2/c
Temperature (K)	293(2)
a, *b*, *c* (Å)	16.820(5), 20.354(7), 9.340(3)
β (°)	103.564(9)
V (Å^3)	3108.5(17) Å
Z	4
Radiation type	MoK_α
μ (mm^{-1})	0.77
Crystal size (mm)	0.07 × 0.06 × 0.02
Data collection	
Diffractometer	Bruker *APEX-3 CCD*
Absorption correction	multi-scan Bruker
No. of measured, independent and observed [$I > 2\sigma(I)$] reflections	22994, 2883, 1448
R_{int}	0.181
$(\sin \theta/\lambda)_{max}$ (Å^{-1})	0.606
Refinement	
$R[F^2 > 2\sigma(F^2)]$, $wR(F^2)$, S	0.138, 0.263, 1.25
No. of reflections	2883
No. of parameters	214
H-atom treatment	H atoms treated by a mixture of independent and constrained refinement
$\Delta\rho_{max}$, $\Delta\rho_{min}$ (e Å^{-3})	0.86, −0.49

Computer programs: APEX3 (Bruker, 2013), SAINT(Bruker, 2013), Bruker SAINT, SHELXS (Sheldrick, 2008), SHELXL (Sheldrick, 2015), Mercury (Macrae, 2020), WinGX (Farrugia, 2012).

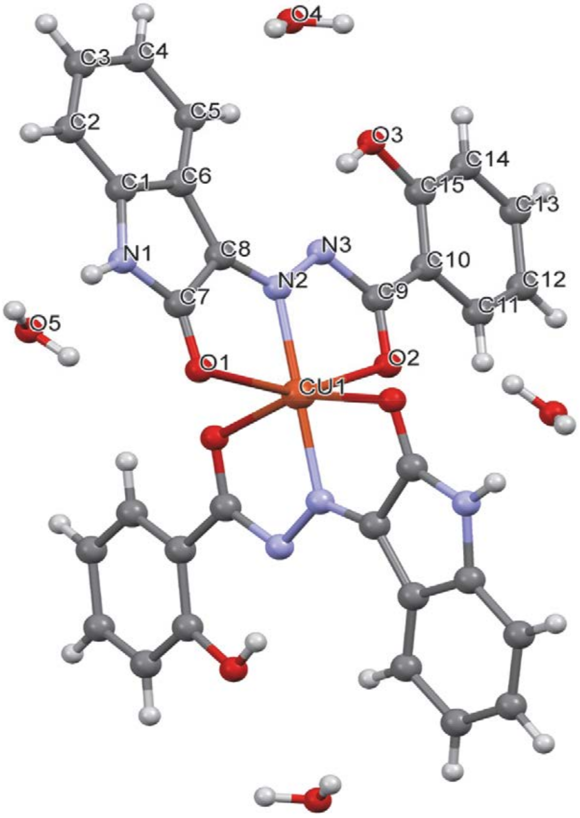

Fig. 1. The assymetric unit of the title compound with the atom numbering scheme.

Table 2. Hydrogen-bond geometry (Å, °).

D—H···*A*	*D*—H	H···*A*	*D*···*A*	*D*—H···*A*
N1—H1···O5	0.86	1.94	2.780(15)	166
O3—H3···N3	0.82	1.82	2.543(11)	146
O5—H5A···O4^{ii}	0.90	2.51	3.09(2)	123.4(12)
O5—H5B···O4^{iii}	0.85	2.53	3.31(2)	152.5(10)

Symmetry codes: (ii) −x + 1/2, y + 1/2, −z + 3/2; (iii) x + 1/2, −y + 3/2,

Table 3. Selected interatomic distances (Å)

C7—O1	1.241(12)	Cu1—N2^i	1.958(7)
C9—O2	1.263(1)	Cu1—N2	1.958(7)
C8—N2	1.275(11)	Cu1—O2	2.09 (7)
N2—N3	1.359(10)	Cu1—O2^i	2.095(7)
C9—N3	1.360(12)	Cu1—O1	2.338(8)
C7—C8	1.495(14)	Cu1—O1^i	2.338(8)
C7—N1	1.346(13)	N1—H1	0.8600
C9—C10	1.465(14)	O3—H3	0.8200

Symmetry code: (i) −x + 1, y.

geometry is given in Table 2. Selected bond lengths and angles are given in Table 3.

In the crystal structure, the intermolecular C–H···O hydrogen bonds (Table 2) link the copper complex molecules and water anions, in which they may be effective in the stabilization of the structure.

3. 3. Stability

The stability of the copper(II) complexes was examined in DMF solution for 24, 48 and 72 hours using a UV-Vis spectroscopy (Figure S9–10). Spectra were recorded at 100 µM concentrations of the complexes. No difference was observed in the spectra of the complexes at the end of 24, 48 and 72 hours. This proves that the complexes are stable in solution.

3. 4. MTT Assays

The cytotoxicities of the complexes against human cancer cell lines, namely lung carcinoma cell line (A549) and breast carcinoma cell line (MCF-7), were investigated utilizing the MTT assay. The same conditions were applied for the positive control, involving the traditional anticancer agent cisplatin. Additionally, to facilitate an additional comparison of cytotoxicity between the complex compounds and cisplatin, evaluation was conducted on the human normal cell line 3T3 (embryonic fibroblast cells). The IC_{50} values for both the complexes and cisplatin were determined using data derived from MTT assays conducted after 24, 48, and 72 hours of incubation, employing various doses spanning from 7.5 to 250 µM, as illustrated in Fig. 2.

The results have demonstrated that, especially in comparison to cisplatin, the $Cu(L^1)_2$ complex exhibits a visibly inhibitory effect on all tested tumor cells in a dose-dependent manner. Although the complex's inhibitory impact on MCF-7 and A549 cell lines is not as pronounced as that of cisplatin ((with IC_{50} values of 182.67 ± 0.01 (24 hours), 38.53 ± 0.11 (48 hours), and 22.40 ± 0.13 (72 hours) for MCF-7; and IC_{50} values of 157.95 ± 0.49 (24 hours), 52.22 ± 0.46 (48 hours), and 26.95 ± 0.30 (72 hours) for A549)), it still displays an effect. Dose-response curves for the $Cu(L^2)_2$ complex against MCF-7 and A549 cancer cell lines after 24, 48, and 72 hours of treatment are presented in Fig. 2. The cytotoxic effect of the $Cu(L^1)_2$ complex on cancer cells is higher than that of the $Cu(L^2)_2$ complex. When compared to the positive control of cisplatin, the complexes exhibit limited inhibition on the 3T3 cell lines over the 24, 48, and 72-hour periods. Moreover, the outcomes indicate the capacity of the complexes to dose-dependently and temporally hinder cellular growth.

Furthermore, the analysis of the cytotoxicity of the complexes and cisplatin (control) on the human normal cell line 3T3, as presented in Fig. 2, underscores the toxicity of both compounds towards cells. At 48 and 72 hours, the complexes exhibited comparable effects (IC_{50} values of 38.53 ± 0.11; 82.21 ± 0.22 and 52.22 ± 0.46; 48.55 ± 0.27, respectively) to those of cisplatin (with IC_{50} values of 32.50 ± 0.02 and 3.65 ± 0.87), albeit not as potent.

Additionally, the cytotoxic selectivity indices (SI)[31] for both the complexes and cisplatin were determined and compiled in Table 4.

Table 4. SI* Values (µM) of Cu(II) complexes obtained with different cell lines for 48 h.

Compounds	3T3/ MCF-7	3T3/A549
$Cu(L^1)_2$	3.95	2.92
$Cu(L^2)_2$	0.27	0.45
Cisplatin	10.80	96.13

*SI, cytotoxic selectivity index (the degree of selectivity between healty cells and cancer cells, expressed as SI = IC_{50} on normal cells/ IC_{50} on cancer cells).

Some of the other notable findings arising from this in vitro cytotoxicity study encompass the incorporation of SI (Selectivity Index) values. These values were calculated with the purpose of assessing the selective impact of the compounds on cancer cells, achieved by juxtaposing the IC_{50} values of the complexes against those exhibited by the normal cell line.[32,33] Despite the fact that the cytotoxic selectivity of the complexes, particularly $Cu(L^1)_2$, does not attain the level observed with cisplatin, the SI values remain above 2 for both cancer cell lines, thereby warranting consideration as an acceptable level of selectivity:

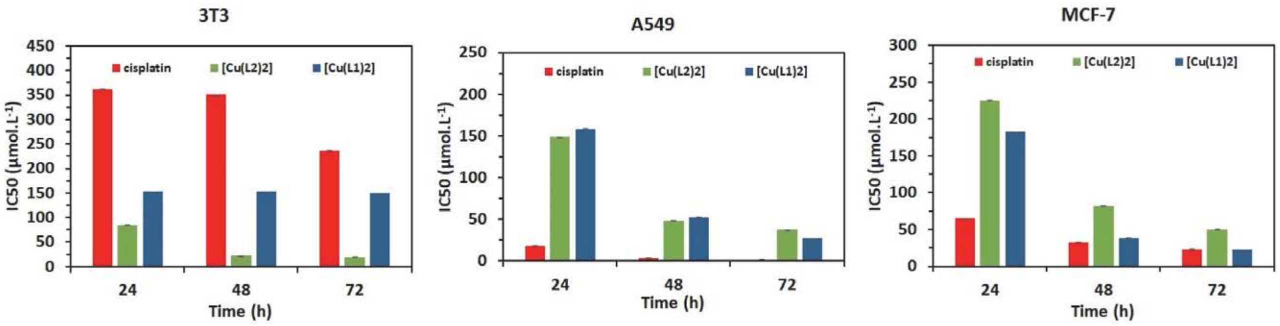

Fig. 2. MTT assay results

SI($_{3T3/A549}$)= 2.92 and 0.45, SI($_{3T3/MCF-7}$)= 3.95 and 0.27. The findings put forth the proposition that the compound's diminished cytotoxicity towards healthy cells, coupled with its moderate cytotoxicity towards cancer cells, augments its viability for the exploration of its potential anticancer effects. Consequently, the compound could potentially induce selective lethality in both cancer cells and healthy cells.[34]

4. Conclusions

In this study, two novel hydrazine-hydrazone ligands were synthesized through the reaction of the isatin moiety with 4-hydroxybenzohydrazide and salicyloylhydrazine. Subsequently, Cu(II) complexes of these ligands were prepared and their structures were investigated using various spectroscopic techniques. Additionally, the crystal structure of the $Cu(L^2)_2$ complex containing the salicyloylhydrazine moiety was elucidated using X-ray crystallography. The cytotoxicities of the obtained complexes against MCF-7 and A549 cancer cells were examined. In studies where cisplatin was utilized as a control, it has been demonstrated that the $Cu(L^1)_2$ complex with the hydroxyl group in the *-para* position exhibits a superior cytotoxic effect against these cancer cells compared to the $Cu(L^2)_2$ complex.

The available spectroscopic data have played a significant role in elucidating the chemical properties and structures of H_2L^1 and H_2L^2 ligands, as well as $Cu(L^1)_2$ and $Cu(L^2)_2$ complexes. The 1H NMR spectra have clearly demonstrated the chemical characteristics of the ligands and provided insights into the coordination mechanisms of the Cu(II) complexes. IR spectra have assisted in determining the coordination changes in the Cu(II) complexes, while magnetic moment data have indicated the high-spin configuration of the mononuclear Cu(II) complexes. Thermal analyses have allowed for the examination of the thermal behavior of the complexes. These results succinctly summarize the key findings of this study. In this context, the combination of spectroscopic and structural data comprehensively explains the chemical properties and structures of H_2L^1, H_2L^2, $Cu(L^1)_2$ and $Cu(L^2)_2$.

The disparity observed in the cytotoxicities of the complexes may potentially stem from the influence of the positioning of the hydroxyl group on the formation of hydrogen bonds within the compounds. The Cu(II) complex with the hydroxyl group in the *-ortho* position could establish stronger hydrogen bonding, whereas *-para* hydroxyl groups might form weaker hydrogen bonds. Consequently, this discrepancy could impact the interaction potential and binding affinities of the compound with target molecules.

In summary, the investigations have evidenced that the $Cu(L^1)_2$ complex exhibits a substantial, selective, concentration-dependent cytotoxic impact, particularly on the viability and proliferation of breast cancer cells. Moreover, in order to validate the anticancer benefits of this study, it is essential to conduct in vivo research.

Acknowledgements

The author acknowledge to Scientific and Technological Research Application and Research Center, Sinop University, Turkey, for the use of the Bruker D8 QUEST diffractometer. Also I extend my sincere gratitude to Sevil Dilara Yeniocak for her invaluable contributions and assistance in my cytotoxicity research, which greatly enriched the quality and depth of my study.

Conflict of interest

The authors declare that they have no conflict of interest.

5. References

1. S. Mishra, P. Singh. *Eur. J. Med. Chem.* **2016**, 124, 500–536. **DOI:**10.1016/j.ejmech.2016.09.055
2. A. Vaidya, S. Jain, P. Jain, N. Tiwari, R. Jain, R. K. Agrawal. *Mini Rev. Med. Chem.* **2016**, 16, 825–845. **DOI:**10.2174/1389557516666160211120835
3. A. El-Faham, M. Farooq, S. N. Khattab, N. Abutaha, M. A. Wadaan, H. A. Ghabbour, H. K. Fun. *Molecules* **2015**, 20, 14638–14655. **DOI:**10.3390/molecules200814638
4. U. Acar Çevik, B. N. Sağlık, C. M. Ardıç, Y. Özkay, Ö. Atlı. *Turk. J. Biochem.* **2018,** 43, 151–158. **DOI:**10.1515/tjb-2018-0201
5. F. Tok, B. N. Sağlık, Y. Özkay, S. Ilgın, Z. A. Kaplancıklı, B. Koçyiğit-Kaymakçıoğlu. *Bioorg. Chem.* **2021**, 114, 105038. **DOI:**10.1016/j.bioorg.2021.105038
6. K. Akdağ, F. Tok, S. Karakuş, Ö. Erdoğan, Ö. Çevik, B. Koçyiğit-Kaymakçıoğlu. *Acta Chim. Slov.* **2022**, 69. **DOI:**10.17344/acsi.2022.7614
7. G. Verma, A. Marella, M. Shaquiquzzaman, M. Akhtar, M. R. Ali, M. M. Alam. *J. Pharm. Bioallied. Sci.* **2014**, 6, 69–80. **DOI:**10.4103/0975-7406.129170
8. J. de Oliveira Carneiro Brum, T. C. França, S. R. LaPlante, J. D. F. Villar, *Mini Rev. Med. Chem.* **2020**, 20, 342–368. **DOI:**10.2174/1389557519666191014142448
9. S. N. Mali, B. R. Thorat, D. R. Gupta, A. Pandey. *Eng. Proc.* **2021**, 11, 21–29. **DOI:**10.3390/ASEC2021-11157
10. N. Metzler-Nolte, H. B. Kraatz, Concepts and models in bioinorganic chemistry. Wiley-VCH, 2006, 443 p.
11. J. M. Berg, Principles of bioinorganic chemistry. 1994, University Science Books.
12. J. F. da Silva, R. J. P. Williams, Book The Biological Chemistry of the Elements, 1991, Clarendon/EditorOxford.
13. B. Kırkan, R. Güp. *Turk. J. Chem.* **2008,** 32, 9–19.
14. R. Güp, B. Kırkan. *Spectrochim. Acta A Mol. Biomol. Spectrosc.* **2005**, 62, 1188–1197. **DOI:**10.1016/j.saa.2005.04.034

15. N. Dilek, B. Güneş, O. Büyükgüngör, R. Güp. *Crystallography Reports* **2013**, 58, 98–104. **DOI:**10.1134/S1063774513010173
16. G. M. Sheldrick. *Acta Crystallogr. Sect. A Found. Adv.* **2008**, 64, 112–122. **DOI:**10.1107/S0108767307043930
17. G. M. Sheldrick, *Acta Crystallographica Section C* **2015**, 71, 3–8. **DOI:**10.1107/S2053273314026370
18. APEX2, Bruker AXS Inc. Madison Wisconsin, USA **2013.**
19. C. F. Macrae, I. Sovago, S. J. Cottrell, P. T. A. Galek, P. McCabe, E. Pidcock, P. A. Wood, *J. Appl. Crystallogr.* **2020**, 53, 226–235. **DOI:**10.1107/S1600576719014092
20. L. J. Farrugia, *J. Appl. Crystallogr*. **2012**, 45, 849–854. **DOI:**10.1107/S0021889812029111
21. T. Mosmann, *J. Immunol. Methods* **1983**, 65, 55–63. **DOI:**10.1016/0022-1759(83)90303-4
22. R. Gup, B. Kırkan, *Spectrochim. Acta Part A* **2005,** 62, 1188–1195. **DOI:**10.1016/j.saa.2005.04.015
23. T. Topal, *Acta Chim. Slov.* **2021,** 68, 88–101. **DOI:**10.17344/acsi.2020.6183
24. T. Topal, H. H. Kart, T. Taslip, E. Karapinar, *Оптика и спектроскопия* **2015**, 118, 897–912. **DOI:**10.7868/S0030403415060227
25. K. Akdağ, F. Tok, S. Karakuş, Ö. Erdoğan, Ö. Çevik, B. Koçyiğit-Kaymakçıoğlu, *Acta Chim. Slov.* **2022,** 69. **DOI:**10.17344/acsi.2022.7614
26. R. Gup, C. Gökçe, N. Dilek, *Supramol. Chem.* **2015,** 27, 629–641. **DOI:**10.1080/10610278.2015.1051978
27. C. Gökçe, N. Dilek, R. Gup, *Inorg. Chim. Acta* **2015,** 432, 213–220. **DOI:**10.1016/j.ica.2015.03.040
28. Z. C. Liu, B. D. Wang, B. Li, Q. Wang, Z. Y. Yang, T. R. Li, Y. Li, *Eur. J. Med. Chem.* **2010,** 45, 5353–5361. **DOI:**10.1016/j.ejmech.2010.08.060
29. S. Ramakrishnan, D. Shakthipriya, E. Suresh, V. S. Periasamy, M. A. Akbarsha, M. Palaniandavar, *Inorg. Chem.* **2011,** 50, 6458–6471. **DOI:**10.1021/ic1024185
30. A. T. López, M. R. A. Luckie, D. M. Otero, V. S. Mendieta, R. Escudero, F. Morales, *J. Chem. Crystallogr.* **2022,** 1–8. **DOI:**10.1007/s10870-021-00893-2
31. A. Koch, P. Tamez, J. Pezzuto, D. Soejarto, *J. Ethnopharmacol.* **2005**, 101, 95–99. **DOI:**10.1016/j.jep.2005.03.011
32. M. Alinaghi, K. Karami, A. Shahpiri, A. A. Momtazi-Borojeni, E. Abdollahi, J. Lipkowski, *J. Mol. Struct.* **2020**, 1219, 128479. **DOI:**10.1016/j.molstruc.2020.128479
33. Z. Shokohi-Pour, H. Chiniforoshan, M. R. Sabzalian, S. A. Esmaeili, A. A. Momtazi-Borojeni, *J. Biomol. Struct. Dyn.* **2018,** 36, 532–549. **DOI:**10.1080/07391102.2017.1287006
34. T. D. Pfister, W. C. Reinhold, K. Agama, S. Gupta, S. A. Khin, R. J. Kinders, Y. Pommier *Mol. Cancer Ther.* **2009**, 8, 1878–1884. **DOI:**10.1158/1535-7163.MCT-09-0016

Povzetek

V prispevku opisujemo sintezo dveh novih hidrazin-hidrazon ligandov s kemijsko reakcijo med izatinom, 4-hidroksibenzohidrazidom in salicilohidrazinom. V nadaljevanju smo pripravili komplekse bakra(II) z novimi ligandi in jih karakterizirali z različnimi spektroskopskimi metodami. S kristalografskimi metodami smo določili strukturo kompleksa Cu(L^2)$_2$ s salicilohidrazinom. V nadaljevanju smo raziskave posvetili citotoksičnim učinkom Cu(II) kompleksov z izatinskimi skupinami. Testirali smo njihovo delovanje na celice pljučnega karcinoma (A549) in raka dojke (MCF-7) z metodo MTT in cisplatino kot pozitivno kontrolo. Ugotavljali smo tudi njihove učinke na normalne človeške celice 3T3. Kompleks Cu(L^1)$_2$ izkazuje znatno inhibicijo tumorskih celic, vendar šibkejšo kot cisplatina. Meritve citotoksičnosti kažejo da je indeks selektivnosti (SI) ustrezen za obe vrsti rakastih celic, kar kaže na potencial za selektivno letalnost. Določili smo kristalno strukturo enega od kompleksov in potrdili prisotnost van der Waalsovih interakcij in vodikovih vezi v pakiranju.